Proceedings of Global Power and Propulsion Society
ISSN-Nr: 2504-4400
GPPS Xi'an21
18th – 20th October, 2021
www.gpps.global

GPPS-TC-2021-0180

THE CALCULATING OF THE TRANSIENT TEMPERATURE FIELD OF THE FIRST STAGE SEGMENT RING OF A GAS TURBINE

Wang Bo
Hangzhou Steam Turbine &Power Group Co., Ltd.
bwangff@sohu.com
Hangzhou, Zhejiang, China

Sui Yongfeng*
Hangzhou Steam Turbine &Power Group Co., Ltd.
*Corresponding author:
suiyf@htc.cn
Hangzhou, Zhejiang, China

Wei Jiaming
Hangzhou Steam Turbine &Power Group Co., Ltd.
weijm@htc.cn
Hangzhou, Zhejiang, China

Chu Peng
Hangzhou Steam Turbine &Power Group Co., Ltd.
chup@htc.cn
Hangzhou, Zhejiang, China

Tu Yao
Hangzhou Steam Turbine &Power Group Co., Ltd.
tuy@htc.cn
Hangzhou, Zhejiang, China

Chi Hongwei
Zhejiang Rancon Turbine Innovation Co., Ltd.
Chihw@htc.cn
Hangzhou, Zhejiang, China

ABSTRACT

In this paper, a rapid method for calculating the transient temperature of the hot components of gas turbines is presented, which contains the following steps: 1. The key factors affecting the heat transfer boundary conditions of the hot component are analyzed, and then link these key factors to gas turbine operation parameters, such as: compressor inlet mass flow, compressor exhaust pressure, turbine inlet gas temperature, etc.. 2. Obtain the gas turbine operation parameters mentioned above at each transient time step. 3. Based on dimensionless criterion number analysis, the external and internal heat transfer boundary conditions of the component at each transient time step are obtained by scaling those at the design point. 4. Load the external and internal heat transfer boundary conditions to the component , and solve the conduction heat transfer at each time step with a commercial CFD code. Using the method above, the transient temperature fields of the first stage segment ring of a gas turbine during a cold state start-load-stop process is calculated. The whole process shows that the transient temperature calculation method is easy to use with the computational cost bearable.

Nomenclature

$\overline{T_{in}}$: the massflow average total temperature of the gas at the turbine inlet, K;
$\overline{T_{s1,out}}$: the massflow average total temperature of the gas at the turbine stator one outlet, K;
$\overline{T_{out}}$: the massflow average total temperature of the gas at the turbine exhaust, K;
$\overline{T_{comp,out}}$: the massflow average total temperature of the air at the compressor outlet, K;
T_{ring} : the total temperature of the gas at the ring segment inlet, K;
Nu_{ex}: Nusselt number of the external side (hot side) gas at a certain location, -;
Re_{ex}: Reynolds number of the external side gas at a certain location, -;
pr_{ex}: Prandtl number of the external side gas at a certain location, function of T_{ring} , -;
h_{ex}: the heat transfer coefficient of the external side gas at a certain location, $W/(m^2 \cdot K)$;
k_{ex}: conductivity of the external side gas at a certain location, function of T_{ring} , $W/(m \cdot K)$;
L: characteristic length of the ring segment, m;
a, b, c, d: constants, -;
$m_{ex,R1}$: the massflow of the external side gas at stage one rotor inlet, kg/s;
A1: cross area of the external side gas flow, m^2 ;
μ_{ex} : dynamic viscosity of the external side gas at a certain location, function of T_{ring} , $Pa \cdot s$;

$m_{comp,in}$: the compressor inlet mass flow, kg/s;
$T_{c,in}$: the coolant inlet temperature for ring segment, K;
$T_{c,out}$: the coolant outlet temperature of ring segment, K;
$T_{c,mean}$: the mean coolant temperature along the cooling hole of the ring segment, K;
h_c : the coolant heat transfer coefficient in the hole of the ring, $W/(m^2 \cdot K)$;
δ_m : equivalent wall thickness of the ring at a certain location, m;
λ_m : conductivity of the metal, function of the metal temperature, $W/(m \cdot K)$;
A : heat transfer area m^2;
m_c : coolant massflow, kg/s;
$c_{p,c}$: specific heat capacity at constant pressure of the coolant at the temperature $T_{c,mean}$, $J/(kg \cdot K)$;
μ_c : dynamic viscosity of the coolant at the temperature $T_{c,mean}$, $Pa \cdot s$;
k_c : conductivity of the coolant at the temperature $T_{c,mean}$, $W/(m \cdot K)$;
transient: values at transient state;
baseload: values at the gas turbine baseload state, or the design point;
ρ : density of the metal , kg/m^3;
c : specific heat capacity of the metal, $J/(kg \cdot K)$.

INTRODUCTION

Gas turbines are widely used nowadays in power plants and distributed energy systems for their quick startup and good performance. Studying carefully the transient temperature and sequentially the stress distribution of gas turbine components during the startup-baseload-trip process is important for the life prediction and evaluation of those components(Luca et al., 2012), and also valuable for the optimization of the startup route of the gas turbine(Shenglong et al., 2019).

Xia simulated the natural convection of water in a container and output the transient temperature distribution in the container (Xia et al., 1998). The results were proved to be very accurate compared to test data. Works by Sondak et al. may be the first ones concerning the transient conjugate heat transfer analysis of gas turbine blades (Sondak et al., 2001). Much research have been done as to the transient conjugate heat transfer analysis in the past 20 years. The transient conjugate heat transfer of air jet impinging over a flat circular disk was numerically studied by Yue-Tzu et al. (Yue-Tzu et al., 2007). An unsteady approach with conjugate heat transfer to simulate the in-flight electrothermal de-icing was presented by Reid et al. (Reid et al., 2012).

As to transient conjugate heat transfer analysis, an intricate problem to be solved is how to quantify the huge disparity in time scales between convection of the fluid domain and conduction of solid domain(He,2011). Meng et al. proposed a "loose coupling" method that solves the fluid flow in a quasi-steady way and solves the heat transfer on fluid boundary and heat conduction in solid in a transient way. The method enables long-time transient solving of conjugate heat transfer to converge much faster (Meng et al.,2017). A novel time-step adaption strategy to deal with the timescale problem that was based on the estimation of the magnitude of the truncation error of the time discretization was developed by Maffulli et al. and the method worked stably on both laminar and turbulent flow conditions (Maffulli et al.,2018).

The transient heat transfer of a gas turbine blade is simulated with the commercial software STAR-CCM+ by Jong-Shang et al., and in their study the fluid domain is simulated as steady state while the solid domain is simulated in transient mode (Jong-Shang et al.,2017).Comparison of the wall heat flux between the simulation and test data shows that the treatment is accurate enough. Dealing with the fluid flow and solid heat conduction separately and successively for transient heat transfer solving is a simplified way that may cause slight deviation for it is not a tight coupling method, but it is efficacious, and practical, especially when the geometry is complicated and the transient time duration is long. Within this method, the heat transfer boundary conditions are obtained through fluid flow analysis firstly, and then load these boundary conditions to the solid heat conduction solving, which is much easier, to get the transient wall temperature. Zhang et al. studied the transient heat transfer of civil-aircraft with this "loose coupling" method, and wall temperature results obtained are then used for transient heat load calculation(Zhang et al., 2010).

A common idea for transient wall heat transfer boundary condition calculation is as follows. Collect the data of the gas turbine system, i.e., the compressor ,the combustor and axial turbine's flow parameters at all the transient state, and extract the needed data and then converse them to heat transfer boundary conditions of the component by step-by-step calculation work. The idea is complicated and tedious, although workable if we can really acquire the data of the whole gas turbine system at all the transient states.

However, at most of the time, we are not lucky enough to acquire these data. Cycle and overall performance calculation provides basic and key parameters of the gas turbine at all the transient time such as the compressor inlet mass flow, compressor exhaust pressure, turbine inlet gas temperature, turbine exhaust gas temperature. By linking these key parameters at steady state of the design point (or base load) with those at each transient state of the gas turbine, we are able to get the transient heat transfer boundary conditions via dimensionless criterion number analysis. Thus a small

collection of the "macroscopic" parameters can help to get all the transient heat transfer boundary conditions for a hot component wall temperature calculation at each transient time step. So a rapid method for calculating the transient wall temperature of the hot components of gas turbines is presented in this paper and then a transient analysis of the first stage segment ring of a gas turbine is completed using the method.

RESULTS AND DISCUSSION

Little public research on segment ring heat transfer analysis can be found(Thomas et al.,2019), one reason is that the cooling features of ring segments are not as complicated or advanced as those of turbine vanes and blades. However, the role of ring segments is important in gas turbines. Segment rings form the outer side of the hot gas path and separates the hot side from the cool side. Thus they are also called heat shields, meaning that they work as shields for turbine vane carriers, which are at the cooled side of the gas turbine and made of metals that are not necessarily high-temperature alloys to save costs.

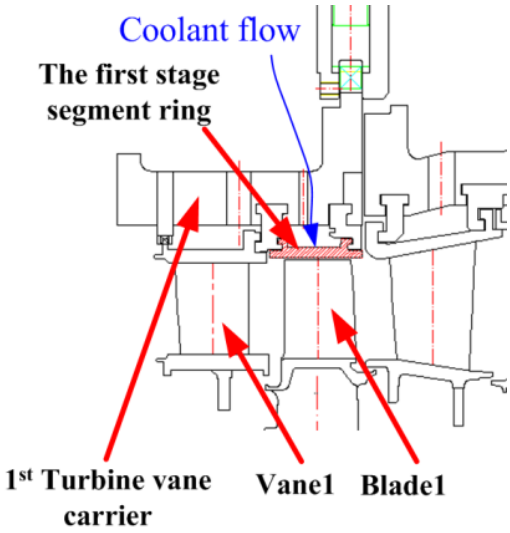

Figure 1 Position of the First Stage Segment Ring in Gas Turbine

Figure 1 shows the position of the first stage ring segments in the gas turbine. Segment rings are assembled to the turbine vane carriers in the gas turbine by the six hooks. The whole ring at the full circle is made of 30 pieces. Figure 2 shows the detailed cooling features of one ring segment. Coolant air bled from the compressor outlet is led to the cavity above the first stage turbine vane carrier. After flowing through the holes at the turbine vane carrier, coolant reaches the cavity above the outer side of the ring, where is usually considered as a good start position for coolant flow calculation of the ring segments. In this cavity, coolant flows uniformly into the drilled holes at the ring segments and cools the segment and afterwards discharges to the hot gas path at the trailing edge.

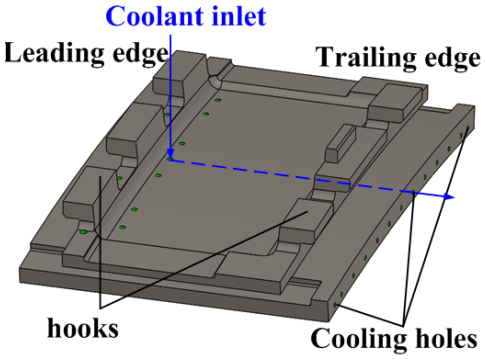

Figure 2 Cooling Features of the First Stage Segment Ring

The time history of reduced rotor speed and reduced compressor inlet massflow during a typical startup-baseload-trip process of the gas turbine is shown in Figure 3. The horizontal axis is broken to show clearly the startup procedure and the trip procedure, which occupy only a small fraction of the whole gas turbine startup-baseload-trip process.

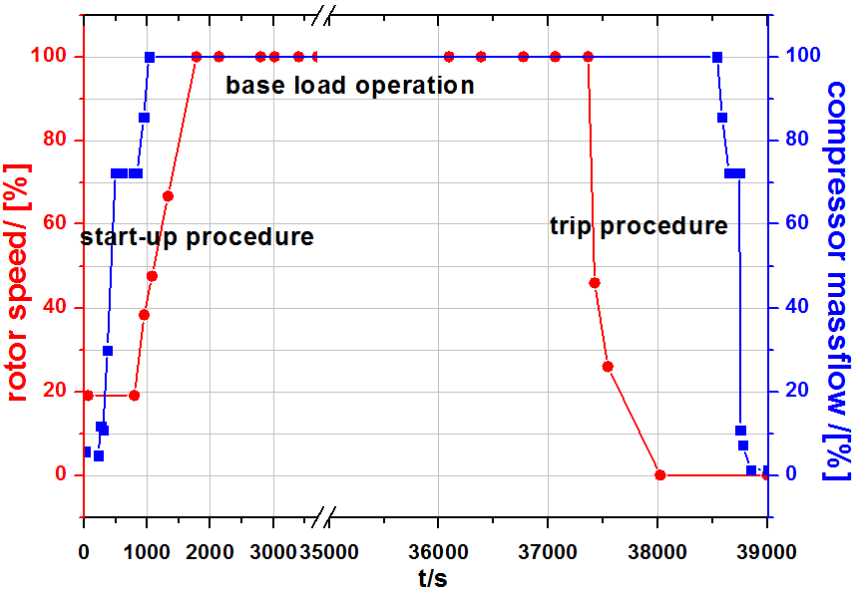

Figure 3 Typical Startup-baseload-trip Process of the Gas Turbine

At the time when t=0 s, the gas turbine is at cool state with a shaft speed of 19% and the compressor massflow is very small. At the time when t=951 s, the igniter acts and the combustor starts to work. Rotor speed rises gradually. In about 30miutes ,the rotor reaches full speed. In one hour, the gas turbine reaches base load (or design point full load) and then works steadily for 10 hours. After that a trip procedure starts, during which the rotor speed decreases and the power output reduces gradually. At the time when t=38024 s, rotor speed gets quite small and reaches 0.05%.The whole start-up-base load-trip cycle lasts 39000 seconds.

External Heat Transfer Boundary Conditions

An overall dimensionless criterion number analysis is needed to get the boundary conditions for the transient wall temperature calculation of the ring segment.

Proper temperature value of the gas at the hot side of the ring should be decided for ring segment wall temperature prediction. Two presumptions are made here. Presumption NO.1: The enthalpy drop from stator one inlet to outlet, keeps the same proportion of the total enthalpy drop from the axial turbine inlet to exhaust at all transient states, thus the gas temperature at the turbine stator one outlet $\overline{T_{s1,out}}$ at each transient state, can be linked to gas temperature at the turbine inlet and gas temperature at the turbine exhaust, as shown in Equation (1). Since parameters at the gas turbine baseload are available, $\overline{T_{s1,out}}$ at each transient state can then be obtained with Equation (1).

$$\frac{(\overline{T_{in}}-\overline{T_{s1,out}})_{transient}}{(\overline{T_{in}}-\overline{T_{out}})_{transient}}=\frac{(\overline{T_{in}}-\overline{T_{s1,out}})_{baseload}}{(\overline{T_{in}}-\overline{T_{out}})_{baseload}} \quad .(1)$$

Mainflow gas temperature is always non-uniform along the radial direction. Gas temperature of ring segment heat transfer should be the value at the maximum radius of stator one outlet , or rotor one inlet. Thus the radial temperature distribution factor (RTDF) at the combustor outlet, or at turbine stage one vanes, is needed for each transient time step. To simplify the solving process, we have presumption NO.2 here: the hot gas temperature distribution pattern along the radial direction , i.e., RTDF at the turbine stator one outlet, keeps the same at all transient states. Thus gas temperature for heat transfer T_{ring}, at the external side ,i.e., the hot side, is calculated by Equations (1) and (2) based on the presumptions we made.

$$\frac{(T_{ring}-\overline{T_{s1,out}})_{transient}}{(\overline{T_{s1,out}}-\overline{T_{comp,out}})_{transient}}=\frac{(T_{ring}-\overline{T_{s1,out}})_{baseload}}{(\overline{T_{s1,out}}-\overline{T_{comp,out}})_{baseload}} \quad . \qquad (2)$$

Usually the external heat transfer coefficient is calculated with the turbulent plate external heat transfer model, as shown in Equations (3) and (4)(Kays W. et al.,1994). Since the Prandtl number of the gas remains almost constant at a very wide temperature range, Equation (4) is then simplified, and thus external side heat transfer coefficient at a transient time step is calculated by Equation (5).

$$Nu_{ex}=a\times Re_{ex}^{b}\times pr_{ex}^{c} \quad .(3)$$

$$h_{ex}=\frac{Nu_{ex}\times k_{ex}}{L} \quad .(4)$$

$$h_{ex} = \frac{d \times (\frac{m_{ex,R1} \times L}{A1 \times \mu_{ex}})^b \times k_{ex}}{L} \propto (m_{ex,R1}^b \times \mu_{ex}^{-b} \times k_{ex}) \ . \quad (5)$$

$$\frac{(m_{ex,R1})transient}{(m_{comp,in})transient} = \frac{(m_{ex,R1})baseload}{(m_{comp,in})baseload} \ . \quad (6)$$

To calculate the massflow of the external side (hot side) gas at a certain location at a certain time step $m_{ex,R1}$ in Equation (5), we need presumption NO.3: The coolant massflow, the seal and leakage massflow for stator one and rotor one keep the same proportions of the compressor inlet mass flow at all transient states, which is rational and widely accepted(Walsh,1998). Based on this presumption, after some simple deduction we get Equation (6) and Equation (10). These equations may not be correct for specific engines at start-up process, which however, will not affect the method proposed here. To improve the precision of the method for a specific gas turbine prediction, what one need to do is to develop one's own heat transfer equations and to substitute the real massflow into the equations for a specific gas turbine or a specific component. However, considerable cost and effort is needed in a gas turbine test.

With the performance and all the details of the gas turbine at the design point baseload already known, the external side gas temperature T_{ring} and heat transfer coefficient h_{ex} at each transient step are obtained by the calculation process above. In this process, instead of a large quantity of data, only four parameters of the gas turbine are needed for each transient state calculation: massflow average total temperature of the gas at the turbine inlet; massflow average total temperature of the gas at the turbine exhaust; massflow average total temperature of the air at the compressor outlet; the compressor inlet mass flow.

Internal Heat Transfer Boundary Conditions

Air temperature and heat transfer coefficient at the internal side ,i.e., the cooled side, are calculated with the almost same method as that of the external side. The coolant for turbine stator one and the first stage segment ring is extracted from the outlet of the compressor and is heated along its flow path, thus its temperature gets a little higher when it reaches the ring. Fortunately, the heating of the coolant is quite small at the gas turbine design point, so we have presumption NO.4 here for internal side heat transfer boundary condition: The inlet coolant temperature for ring segments equals the air temperature at the compressor outlet at all transient states. Mean temperature of coolant at the cooling hole inlet and outlet should be used as the fluid temperature at the internal side of the ring and to decide physical properties.

After entering the holes at the ring segment, coolant is heated gradually in when it flows from the leading edge to the trailing edge. The mean temperature and the outlet temperature of the coolant inside the hole, and the heat transfer coefficient at the internal side of the ring are calculated by Equations (7)~(10) (Yang Shiming. et al.,2006), which is an iterative solving process.

$$T_{c,out} = T_{c,in} + (\frac{T_{ring} - T_{c,mean}}{\frac{1}{h_{ex}} + \frac{1}{h_c} + \frac{\delta_m}{\lambda_m}}) \times A / m_c / c_{p,c} \ . \quad (7)$$

$$T_{c,mean} = (T_{c,out} + T_{c,in})/2 \ . \quad (8)$$

$$h_c \propto (m_c^n \times \mu_c^{-n} \times k_c) \ . \quad (9)$$

$$\frac{(m_c)transient}{(m_{comp,in})transient} = \frac{(m_c)baseload}{(m_{comp,in})baseload} \ . \quad (10)$$

For the first try, we can preset the conductivity of the metal to be a constant and the physical properties of the coolant such as $c_{p,c}$, μ_c and k_c to be decided by the inlet temperature, which will make the solving process much easier. And for the second time, a more precise setting of these parameters can be obtained. It is proved that after two or three times' iteration, the wall temperature prediction of the ring segment would be satisfactory enough for a typical steady state solving.

In the calculating process above, only three parameters of the gas turbine at each transient step are needed: the external side gas temperature T_{ring}, which is known already ; the massflow average total temperature of the air at the compressor outlet; the compressor inlet mass flow.

Since the most important work, i.e., deciding the heat transfer boundary conditions at every transient step, is already finished, now the flowchart to present the method to calculate the transient temperature of a hot component of a gas turbine proposed in this paper is shown in Figure 4.

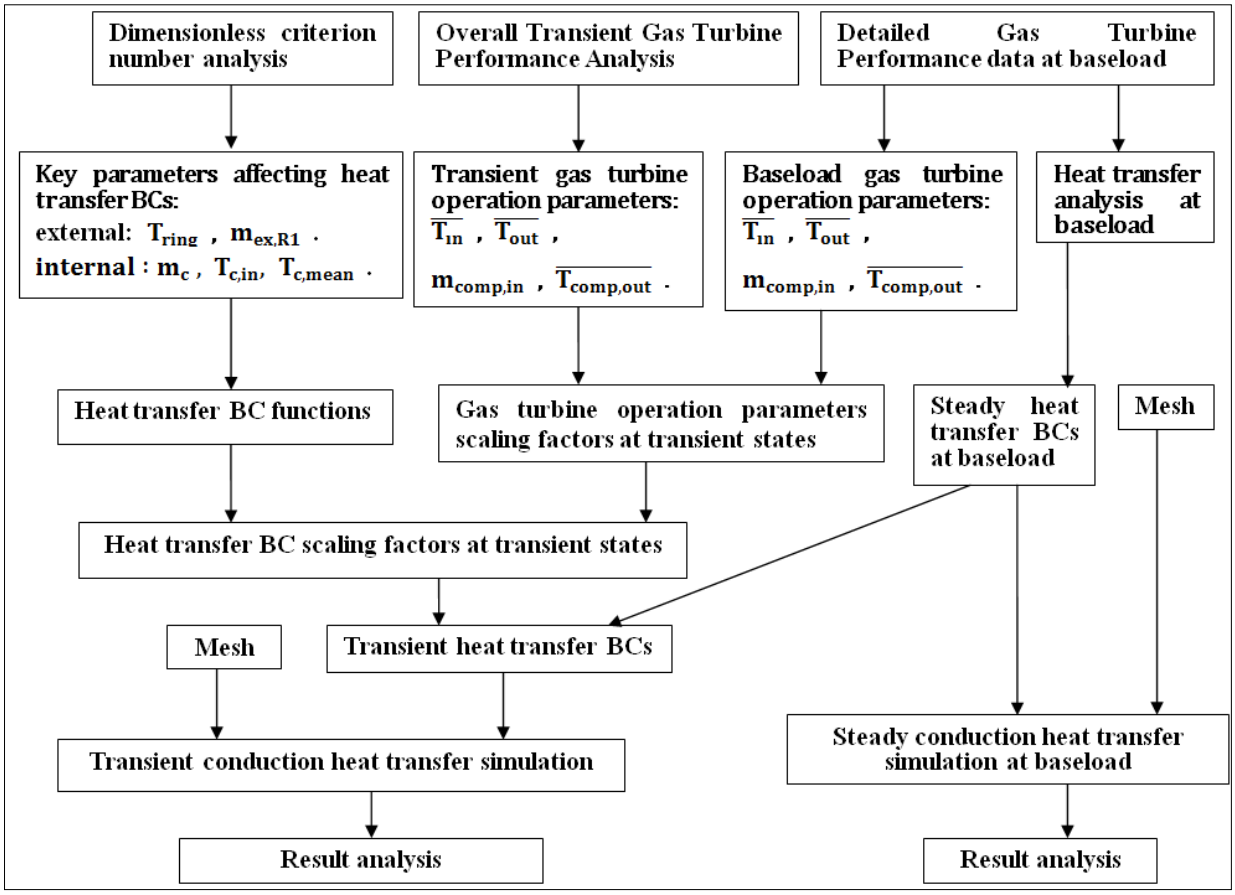

Figure 4 Flowchart of the Method

Calculation of the Transient Temperature of the Ring Segment

Load the external side and internal side heat transfer boundary conditions to the transient FEM temperature calculation, we can get the ring segment wall temperature at each transient time step finally. ANSYS-CFX v19.1 is used to solve the solid domain conduction equations, as shown in Equation (11).The transient scheme used is Second Order Backward Euler method. The maximum number of Coefficient Loops is set to be 10 and the minimum to be 1.

$$\frac{\partial}{\partial x}\left(\lambda_m \frac{\partial T}{\partial x}\right) + \frac{\partial}{\partial y}\left(\lambda_m \frac{\partial T}{\partial y}\right) + \frac{\partial}{\partial z}\left(\lambda_m \frac{\partial T}{\partial z}\right) = \rho c \frac{\partial T}{\partial t} \quad . \quad (11)$$

Mesh independence is done for steady simulation before the transient simulation analysis is started. It is found that the results are not sensitive to mesh setup or the number of elements of the mesh, for the equation we are solving numerically is a solid conduction equation and is much easier than a fluid equation solving. Mesh used for transient simulation in this paper is shown in Figure 5. The number of total elements is 2.47 million.

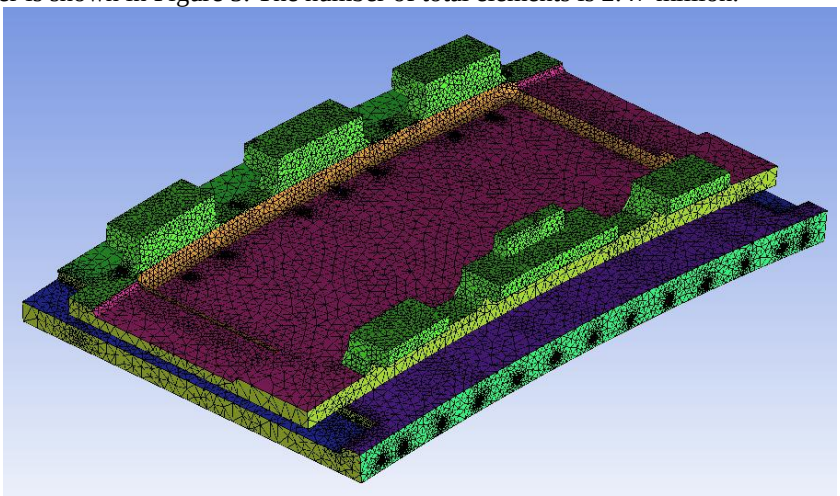

Figure 5 Mesh for Transient Simulation

Three repeated startup-running-shutdown cycles of the gas turbine are unified as one continuous routine. By repeating the start-up cycle three times, we can check the transient temperature results in each single cycle and at each transient time step.

The precision of the method we proposed in this paper depends mainly on the precision of the heat transfer BCs, because solving the conduction heat transfer equations by FEM method is quite common now and can be very accurate, even for transient analysis. The only issue that comes next is how to set the transient time step. In the CFX-pre, as shown in Figure 6, we established four sets of time steps for transient solution to check and to choose the best time step setup for the solver. In timestep setup scheme1, during the full load steady running process of the gas turbine, i.e., physical time from 3693s to 36093s, 42693s to 75093s, 81693s to 114093s ,which is significantly long physical time, few time steps for solving are chosen so as to save CPU time. The total number of time steps for solving is 963. Wang et al. studied the Fourier number and Biot number 's influence on the convergence speed and convergency(Wang et al.,2019). According to this study, we have a better time step setup. Thus in timestep setup scheme 2, number of the timesteps in the full load steady running process of the gas turbine is increased to get more accurate information of the ring wall temperature. In timestep setup scheme 2, the total number of time steps for solving is increased a lot and reaches 3996. The results show that increasing the number of timesteps in the long plat state of the gas turbine does get a better solution for transient analysis results. In timestep setup scheme 3, more detailed timesteps are added to during the startup process and the shutdown process. In timestep setup scheme 3, the total number of time steps for solving is increased to 4143. In timestep setup scheme 4, we use the "Adaptive" time step setup in CFX-Solve, where the maximum time step is set to 500 seconds and the minimum 0.04 second. Within the "Adaptive timestep setup", timestep size will change automatically and dynamically within 0.04s~500s depending on the convergence criteria or Courant number. In timestep setup scheme 4, it is found that the total number of time steps for solving decided by the solver is 718 after the solving process is completed.

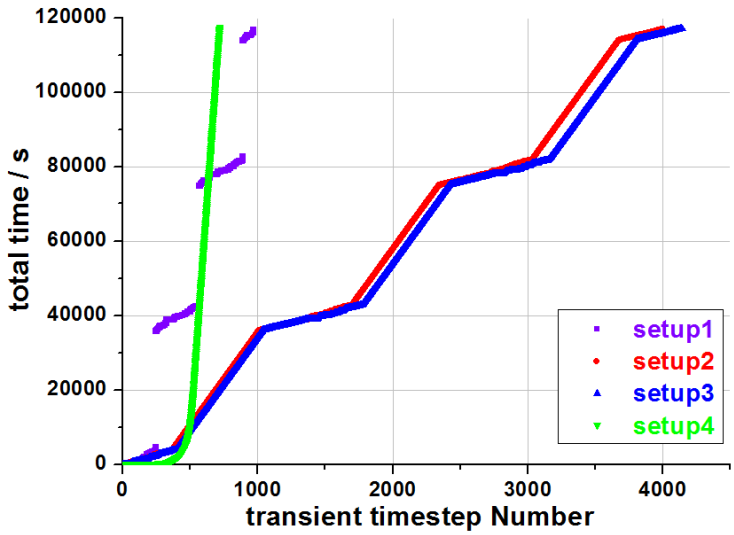

Figure 6 Four Transient Timestep Setup Schemes in CFX-Pre

Residual history plots during the transient analysis solution process corresponding to the four timestep setup schemes are shown in Figure 7. As shown in the figure, timestep setup scheme3 gets the best convergence and could make the thermal energy equation solving root mean square (RMS) residual converged to 1e-5 at all the transient time steps, while scheme1 gets the best convergence. Scheme2 is better than scheme1 and could make the thermal energy equation solving RMS residual converged to 1e-4. Scheme4 needs the least number of time steps, meaning the least CPU time, while the RMS residual is kept lower than 1e-5.

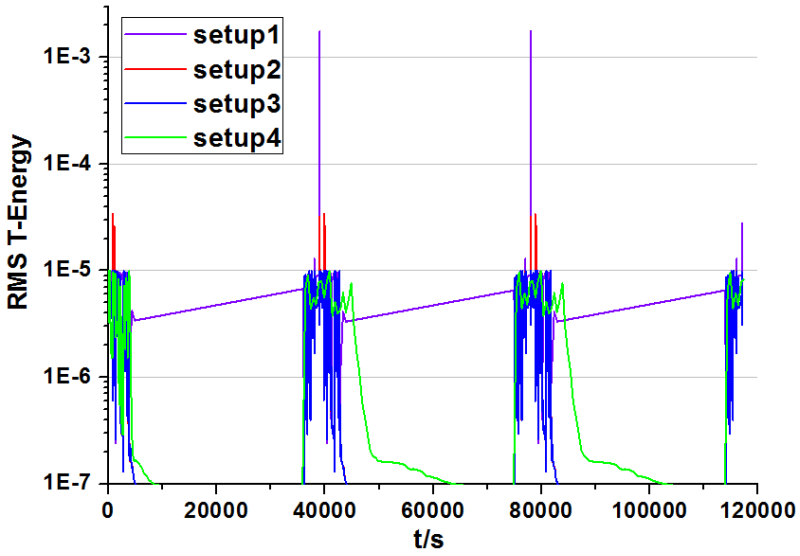

Figure 7　Residual History Plots in CFX-Solve

The area average temperature of the hot side of the ring segment obtained with the four timestep setup schemes is shown in Figure 8. It is observed that even though different timestep setup causes the thermal energy equation solving RMS residuals to vary greatly, the ring segment hot side temperature results are almost the same with a maximum absolute temperature disparity of only ±10K, which is observed at other faces of the ring, too. So we can say that the CFX solver is robust enough for transient solid wall temperature prediction when solid domain heat conduction is not coupled with fluid flow solving.

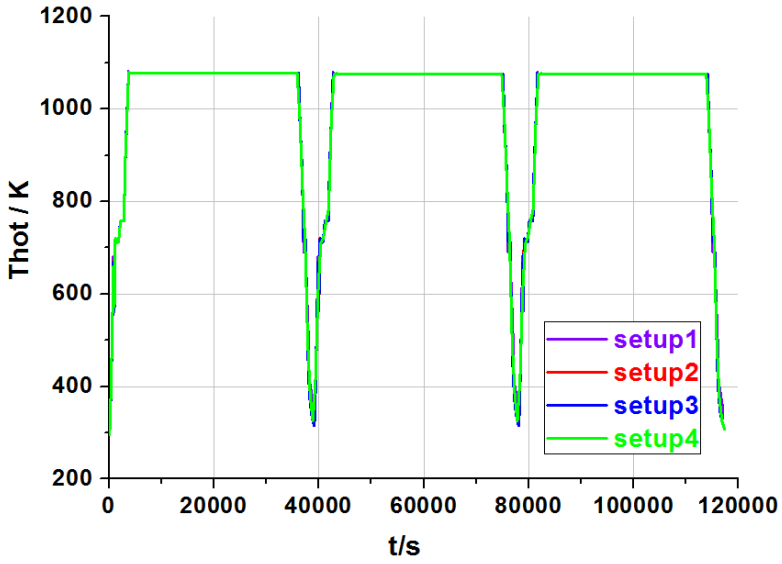

Figure 8　Area Average Wall Temperature of the Hot Side

Result Analysis

The transient cooled side wall temperature of the ring segment obtained with timestep setup scheme 4 is shown in Figure 9. Solid wall temperature evolution repeats itself three times exactly corresponding to the three repeated startup-baseload-shutdown cycles, indicating that the transient temperature prediction is rational. Comparison of temperature of the cooled side, the cooling hole wall and the hot side of the ring segment at transient and steady state is shown in Figure 10. In this figure, the horizontal axis is broken to show clearly the startup procedure and the trip procedure. Ring temperature at steady state and at transient state show good agreement, meaning that the time intervals for heat transfer boundary condition to change from one to another are long enough to allow the wall temperature to become steady. Thus in each transient step, the heat transfer behavior can be treated approximately as quasi-steady-state.

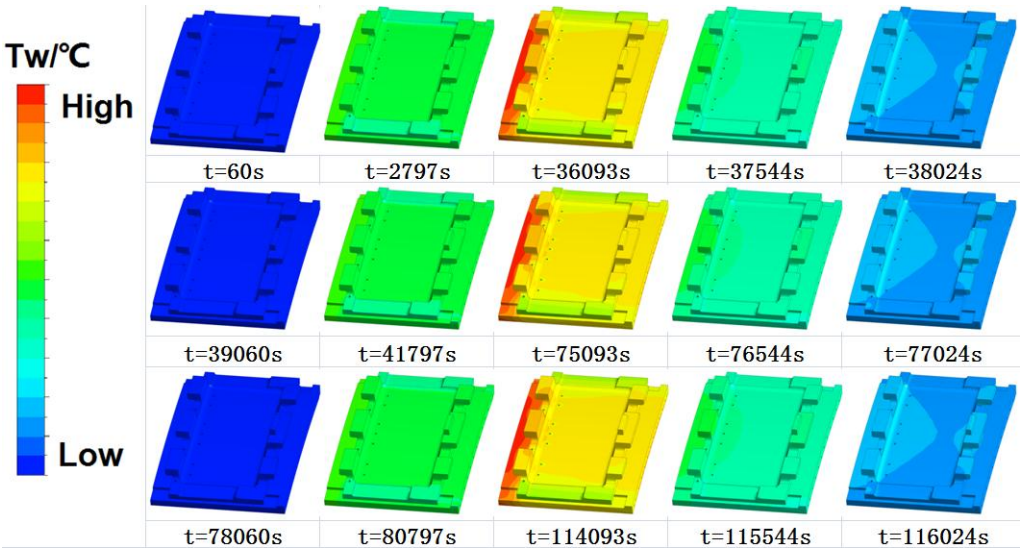

Figure 9 Transient Ring Segment Wall Temperature

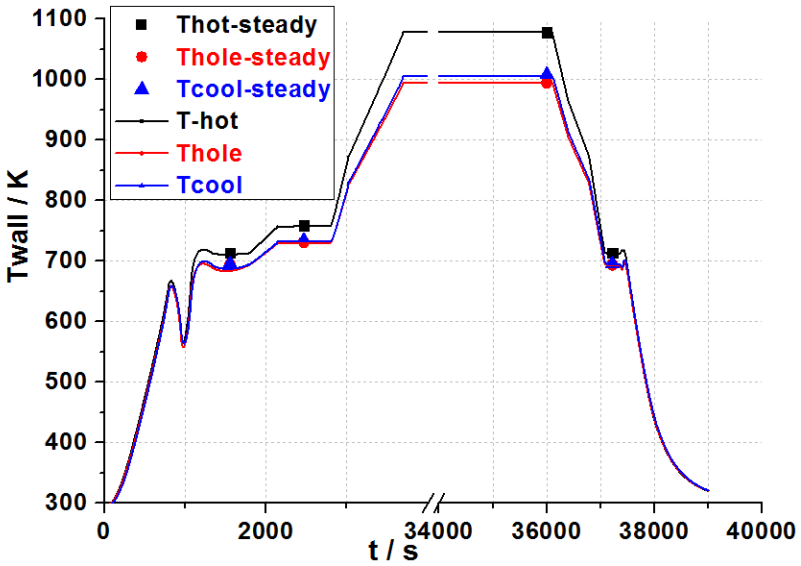

Figure 10 Transient Wall Temperature vs. Steady Wall Temperature

Transient wall temperature can give valuable data for the life prediction and evaluation of ring segments, and also valuable for the optimization of the startup route of the gas turbine.

CONCLUSIONS

1) A rapid method based on the "loose coupling" approach for predicting the transient wall temperature of gas turbine hot components is presented in this paper, within which the heat transfer boundary conditions for solid conduction solving at each transient time step can be obtained easily by a few key "macroscopic" parameters of the gas turbine, saving considerable time and effort for, especially, long-time transient analysis.

2) Transient analysis of the first stage segment ring of the gas turbine is completed using the method in this paper, proving that the method works well with computational cost bearable.

3) The ring segment wall heat transfer behavior in each transient step of a typical startup-baseload-trip process can be treated as quasi-steady.

REFERENCES

He, L. . (2011). Unsteady Conjugate Heat Transfer Modeling. *ASME Turbo Expo: Power for Land, Sea, & Air,2011*.

Jong-Shang Liu, Mark C. Morris, Malak F. Malak, et al. (2017).Comparison of 3d unsteady transient conjugate heat transfer analysis on a high pressure cooled turbine stage with experimental data. *Proceedings of ASME Turbo Expo 2017: Turbomachinery Technical Conference and Exposition.*

Kays W. , Crawford. M. (1994). *Convective Heat And Mass Transfer*. 3rd ed. McGraw-Hill Publications, pp. 274-284.

Luca Bozzi, Andrea Perrone, Luca Giacobone. (2012). Procedure for calculation of component thermal loads for running clearances of heavy-duty gas turbines. *ASME Turbo Expo 2012*.

Meng Fanchao, Dong Sujun, Jiang Hongsheng, et a1(2017). A fast algorithm for long-term fluid-solid conjugate heat transfer process. *Journal of Beijing University of Aeronautics and Astronautics*, 43(6),pp.1224-1230.

R. Maffulli, L. He, P. Stein. , et al. (2018). Fast conjugate heat transfer simulation of long transient flexible operations using adaptive time stepping. *Proceedings of ASME Turbo Expo 2018 Turbomachinery Technical Conference and Exposition,2018.*

Reid, Thomas, Baruzzi, Guido, Habashi, et al. (2012). FENSAP-ICE: Unsteady conjugate heat transfer simulation of electrothermal de-icing. *Journal of Aircraft*, 49, pp.1101-1109.

Shenglong LIU, Xiaorong WANG, Qiangfeng CHEN, et al. (2019). Optimization of Startup Process of Turbine in Combined Cycle Unit. *International Conference on Power Engineering-2019.*

Sondak.D. L. ,Dorney.D. J. . (2001). Conjugate Unsteady Heat Transfer Simulation in a Turbine Stage. *De Gruyter 2001.*

Thomas Wimmer, Tobias Ruehmer, York Mick . (2019). Experimental and numerical investigation on an additively manufactured gas turbine ring segment with an in-wall cooling scheme. *Proceedings of ASME Turbo Expo 2019: Turbomachinery Technical Conference and Exposition,2019.*

Walsh, P. P. , P. Fletcher . (1998).*Gas turbine performance.* Oxford :Wiley-Blackwell. , pp. 229-230.

Wang Yangli, Jin Haiyan.(2006). Effect of calculation parameters on convergence speed of one-dimensional transient heat transfer series solution *Journal of North China Electric Power University*,33(4),pp.99-101.

Xia J L , Smith B L , Yadigaroglu G , et al. (1998). Numerical and experimental study of transient turbulent natural convection in a horizontal cylindrical container. *International Journal of Heat & Mass Transfer,* 41(22), pp.3635-3645.

Yang Shiming, Tao Wenquan. (2006). Heat Transfer. Beijing: Higher Education Press., pp. 246-252.

Yue-Tzu Yang, Shiang-Yi Tsai.(2007).Numerical study of transient conjugate heat transfer of a turbulent impinging jet. *International Journal of Heat and Mass Transfer* ,50 (2007), pp. 799–807.

Zhang Qiu, Jiang Yanlong, She Yangzi, et al. (2010). Numerical calculation of transient temperature distribution of civil aircraft cabin. *Journal of Nanjing University of Aeronautics& Astronautics*,42(4),pp.466-471.